13th ewtec 2019 Proceedings of the 13th European Wave and Tidal Energy Conference 1-6 Sept 2019, Naples, Italy

A case study of high frequency AD2CP measurements for tidal site characterization in Banks Straits, Tasmania, Australia

Larissa Perez, Remo Cossu, Irene Penesis, Alistair Grinham, Jean R. Nader and Camille Couzi

Abstract— **Acoustic Doppler Current Profilers (ADCPs) are the state-of-the-art instrumentation to characterize tidal sites. However, more recently, advanced technology instruments – such as Nortek Signature AD2CPs – allow for higher frequency measurements with lower noise levels. These instruments provide turbine developers with important information regarding small-scale turbulence in highly energetic tidal channels and, therefore, contribute to the design of more resistant structures, reducing the unsteady loading on turbine blades. Here we report and compare measurements taken with an RDI Workhorse 300 kHz ADCP and a Nortek Signature 1000 kHz AD2CPs deployed in two different locations within Banks Strait, Australia, between March and July 2018. Flow velocity and direction statistics as well as power densities are assessed. Turbulence measurements performed by the Signature indicate significant wave-current interaction at the site, which was not detected by the WorkHorse. Results indicate substantial spatial variability in tidal resource between two measurement locations, with mean power densities varying between less than 100 W/m² at one location to over 900 W/m² at the most energetic site. The AD2CP instrument proved to be more efficient to characterize the site and is able to overachieve requirements set by the EMEC guidelines, since this technology allows for simultaneous velocity and turbulence measurements. To our knowledge, this is the longest field measurement done using this technology and its results could represent a significant advance in tidal site characterization and provide advanced information to turbine developers at an early stage.**

Keywords— *Acoustic Doppler current profiler (ADCP),* **AD2CP, tidal currents, tidal energy, turbulence, wave-current interaction, tidal-stream resource characterisation.**

ID number: 1538 – Tidal resource characterization. The project is co-funded by the Australian Renewable Agency (ARENA) through the Advancing Renewables Programme (grant G00902), the Australian Maritime College, (University of Tasmania), the University of Queensland, CSIRO Oceans and Atmosphere, CSIRO Energy, our industry partners, SIMEC Atlantis Energy and MAKO Tidal Turbines and our international collaborators Prof. Richard Karstens from Acadia University, Canada, and Dr Matt Lewis from Bangor University, UK.

L. Perez is with the Faculty of Engineering, Architecture and Information Technology, The University of Queensland, Australia (e-mail: l.perez@uqconnect.edu.au).

R. Cossu is with the Faculty of Engineering, Architecture and Information Technology, The University of Queensland, Australia (e-mail: r.cossu@uq.edu.au).

I. Penesis is with the Australian Maritime College, University of Tasmania, Australia (e-mail: i.penesis@utas.edu.au).

A. Grinham is with the Faculty of Engineering, Architecture and Information Technology, The University of Queensland, Australia (e-mail: a.grinham@uq.edu.au).

J. R. Nader is with the Australian Maritime College, University of Tasmania, Australia (e-mail: jeanroch.nader@utas.edu.au).

C. Couzi is with the Australian Maritime College, University of Tasmania, Australia (e-mail: camille.couzi@utas.edu.au).

I. Introduction

RELYING on finite resources in order to generate electricity may be risky, expensive and highly damaging to the environment. Nonetheless, fossil fuels still represent over 85% of the electricity generated in Australia [1], enhancing the need to shift and invest in other energy sources. Thus, ocean renewable energies are currently considered and investigated as an alternative energy resource [2]. The work presented here is part of the AUSTEn Project, with the main goal to assess Australia's tidal energy resources using several field campaigns at different locations as well as the economic and technical feasibility of implementing this technology in the country. One of the "candidate sites" for tidal energy is the area around Banks Strait, a highly energetic tidal channel located between Clarke Island and Northeast Tasmania, connecting Bass Strait and the Tasman Sea.

ADCPs have been introduced in the 1980s and are now widely utilized in order to characterize currents velocities and turbulence along depth profiles. However, instruments most commonly used are limited to low frequency measurements, thereby not capturing small-scale turbulence fluctuations. Alternatively, Acoustic Doppler Velocimeters (ADVs) are typically capable of measuring at higher sampling rates and take in consideration a smaller sampling volume, therefore being able to provide more detailed turbulence data [3]. Although ADVs can offer high frequency measurements, their deployment period is often limited due to battery use and these instruments are unable to provide velocity profiles across the water column. Hence, these instruments provide very limited information on seasonal

variability information. More recently, advanced technology instruments, such as Nortek Signature AD2CPs, allow for high frequency measurements with lower noise levels – when compared to classic ADCPs – and more extensive deployments. In addition, Signature AD2CPs present the ability to interleave acoustic sampling with different configurations [4], which allows for a richer data set from a single deployment. The European Marine Energy Centre (EMEC) guidelines set international standards for tidal stream energy site assessments and recommends three months of velocity data collection, with the requirement of a minimum duration of one month. Amongst other variables, some of the expected outputs are velocities in all three directions, average velocities and turbulence intensities. Since the new AD2CP technology is capable of measuring simultaneously both velocity and turbulence during long deployments, this instrument can, therefore, fulfil more of the listed requirements, compared to classic ADCPs.

Surface gravity waves and flow turbulence are some of the main contributors to turbine blades fatigue. Waves influence current velocities and, hence, affect extracted power and blade loading [5]. Studies conducted in other tidal stream energy sites, such as Fall of Warness, Cook Strait and Pampol-Brehat have reported wave-current interaction [6], [7], [8]. A wide range of experiments have been conducted in order to better investigate the impact of waves and turbulence on tidal turbine performance [5], [9], [10], [11], [12], [13], [14]. The interference caused by wave and turbulence may negatively impact tidal turbine performance, as it results in an increase of power and thrust fluctuations. Therefore, wave-current interaction in tidal-stream energy sites still represents a significant uncertainty for tidal resource characterization and turbines power production.

Here we report and compare measurements taken using a Teledyne RDI Workhorse 300 kHz ADCP and a Nortek Signature 1000 kHz deployed in different locations within Banks Strait. Instruments were deployed between March and July 2018, therefore allowing for observations of seasonal variations of flow characteristics and strong wind events. Initially tidal resource is characterized based on velocity and turbulence measurements and velocity profile power laws and power densities are estimated. Wave-current interaction is found to be an important characteristic at the site and is discussed. Finally, information provided by both instruments is compared.

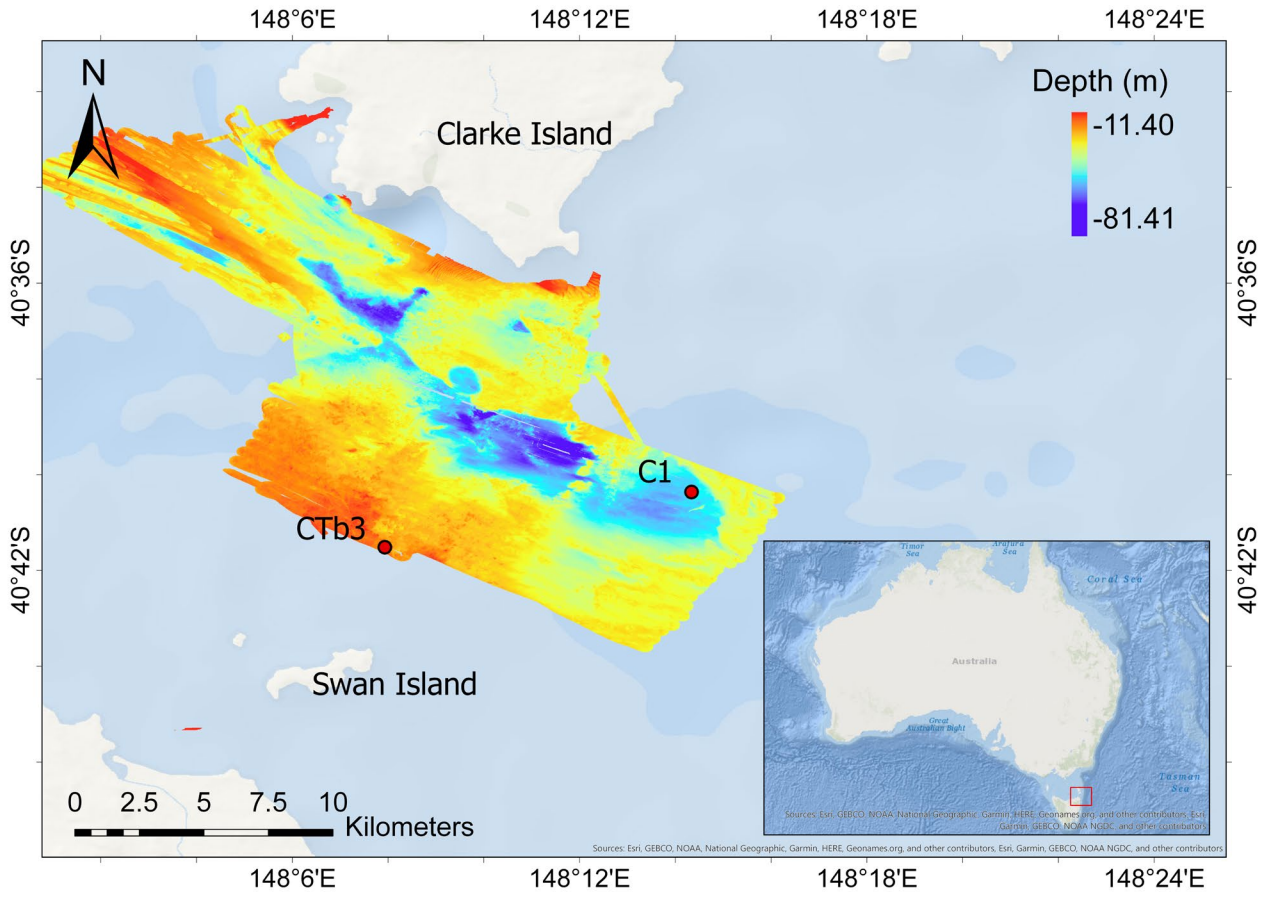

Fig. 1. Banks Strait, located in Northeast Tasmania. RDI ADCP (C1) was deployed in a deep pocket in the approximate centre of the channel and the Nortek Signature (CTb3) was located in the Southern part of the channel, near Swan Island, in a shallower area. Both instruments were deployed from March – July 2018, allowing for an extensive data set collection.

II. METHODOLOGY

A. Site description

Banks Strait is a highly energetic tidal channel in Northeast Tasmania, Australia, located in the Eastern side of Bass Strait, between Clarke and Swan Islands. Fig. 1 illustrates the site and its bathymetry as well as the deployment location of both instruments. The channel is approximately 16 km wide and its depth varies between 30 and 40 m, with a few deeper pockets reaching 70m. Data from the open-access Australian Wave Energy Atlas (AWavEA) made available through the Australian Renewable Energy Mapping Infrastructure (AREMI) suggests significant wave heights varying mostly between 1 and 2 m, with maximum heights of approximately 5-6 m. Its dominant tidal harmonics constituent is M2, followed by N2, S2 and MSF. Models have previously characterized this site as one of the highest tidal current speeds in Australia, routinely reaching 2.6 m/s [15]. Regarding tidal energy potential, it presents a temporal mean tidal stream energy density of between 600 and 2000 W/m² [16].

B. Instruments configurations

The data discussed in this work were collected using two different generations ADCP devices. The Teledyne RDI Workhorse 300 kHz (C1), deployed in the approximate centre of the channel, in approximately 57 meters (40° 40' 21.72" S, 148° 14' 20.40" E, Fig. 1). This instrument was set to measure and time-average velocities with 50 pings during 5-minute periods with break intervals of same length, with a blanking distance of 1.76 m and cell size of 2 m. The Nortek Signature 1000 kHz (CTb3) was located in an area approximately 33 meters deep, in the Southern part of the channel, near Swan Island (40°41'30.98" S, 148° 7'55.60" E, Fig. 1). As allowed by the AD2CP technology, this instrument was set in two different configurations to interleave during the complete deployment period, in order to measure both current velocities and turbulence. The first configuration set the instrument to measure current velocities with break intervals of 5 minutes, with 0.1 m blanking distance and 1 m deep cells. The second configuration was to measure turbulence, in which the instrument was set to sample at 8 Hz during 15-minute bursts and in-between intervals of 15 minutes with 0.5 m cell size. In both configurations, the instrument was using its four 25°-slanted beams.

C. Data quality control

For the RDI instrument, data quality procedure consisted of three steps: i) removing data points from cells above the water surface, ii) removal of the top 15% of the water column in order to avoid side lobe interference as well as high velocities caused by waves and iii) removal of possible outliers based three times the velocity standard deviation threshold.

For the Signature 1000, data points with less than 50% beam correlation were removed. In order to avoid low signal strength and high spikes caused by signal interference, a minimum amplitude of 30dB with maximum spikes of 35dB was set. To avoid side lobe interference, the top 10% of the water column was removed. Finally, similarly to the RDI data processing, data from cells above the water surface and possible outliers were also removed.

D. Turbulence signal processing

Here we present turbulence data measured by the AD2CP instrument. To better assess turbulence information and identify frequencies of the energy containing eddies, the high frequency velocity signal was converted from the time domain to the frequency domain based on Welch's periodogram method. This method uses a Fast Fourier Transform, dividing the signal in specified segments multiplied by a windowing function in order to improve frequency resolution, resulting in a power density spectrum.

III. VELOCITY TIME-SERIES CHARACTERIZATION AND STATISTICAL RESULTS

According to data made publicly available by the Australian Bureau of Meteorology, during this time of the year, average wind speeds vary between 23 – 29 km/h, with maximums reaching over 60 km/h. Wind speeds have exceeded 35 km/h during over 20% of the deployment period. Temperatures vary mostly between 20.5°C in March and 8.4°C in July.

Fig. 2 shows flow direction at approximately 15m above the bottom. This is the hub height of a Seagen tidal turbine, and it will be referred to as hub height from now on. Tidal currents are nearly rectilinear at location C1, flowing to approximate Southeast during ebb tide (~ 110.97°) and Northwest during flood tide (~ 272.82°). Nonetheless, at location CTb3 currents present a higher directional difference, flowing to ~ 99.22° during ebb tide and ~ 305.33° during flood tide. Directional asymmetry shows the deviation of the flow from a straight line and is defined here by $|\theta_{flood} - \theta_{ebb} - 180°|$. Ebb and flood directional asymmetry are of 18.15° and 26.11° for C1 and CTb3 respectively.

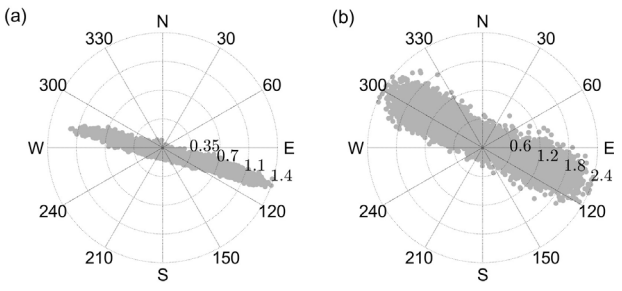

Fig. 2. Flow direction at hub height (~15 above the bottom) at (a) C1 and (b) CTb3.

At C1, most velocities range from 0.5 – 1 m/s, while at CTb3 majority of flow velocities vary from 0.75 – 1.25 m/s (Fig. 3). The analysis in this work will focus mostly on ebb and flood events, when flow velocities are higher and more significant for tidal stream energy assessment. Hence, the 30% lowest velocities were classified as slack conditions and discarded for the calculations of maximum and mean velocities, as well as for the power law estimates. At C1, maximum velocities reached approximately 1.55 m/s during ebb tide. Due to its shallower depth, CTb3 presented higher velocities, with maximum values reaching approximately 3.20 m/s both during ebb and flood tide. Table I summarizes statistical results from the complete data set for both locations. Time averaged profiles for three different flow conditions at hub height are plotted in Fig. 4. To better assess different flow conditions at the sites, hub height velocities were split into three cases: low, medium and high flow speeds based at the velocity at hub height.

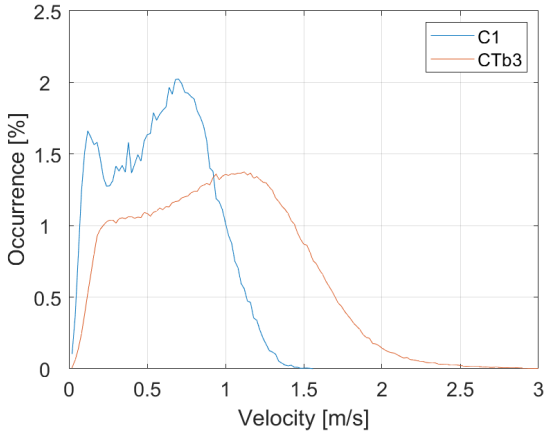

Fig. 3. Flow velocity occurrence curves for both measurement locations.

Fig. 5 shows the average speed profiles for ebb and flood tides for both instruments. Ebb and flood tides were defined based on flow direction. Average velocities are considerably higher at CTb3, reaching over 1.2 m/s both during flood and ebb tides, compared to C1, where average velocities reach approximately 0.7 m/s. The α coefficient from the power law for each profile was calculated based on the model equation:

$$V = Vo(z/d)^{1/\alpha} \quad (1)$$

where V is the average velocity, Vo is the velocity at the surface, z is the height above sensor, d is the location depth and α is the power law coefficient.

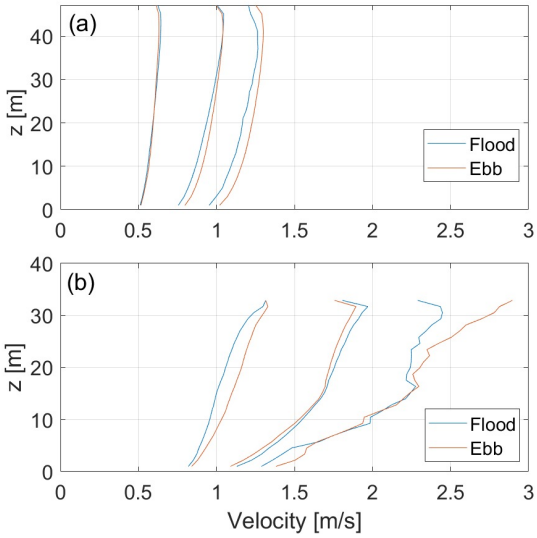

Fig. 4. Time averaged flow velocity profiles for three different cases at C1 (a) and CTb3 (b) based at hub height velocity. In (a), low flow velocities at hub height range from 0.5 – 0.7 m/s, medium velocities from 0.9 – 1.1 and high velocities 1.2 – 1.4 m/s. In (b) low flow hub height velocities range from 0.9 – 1.1 m/s, medium velocities from 1.6 – 1.8 m/s and high velocities from 2.3 – 2.5 m/s.

The power density of a site can be determined by estimating the kinetic energy present within the flow using:

$$P = \frac{1}{2}\rho V^3 \quad (2)$$

where P is the estimated power density (W/m²), ρ is the sea water density (~1025 kg/m³) and V is the velocity of the flow (m/s). Results for maximum and mean power density for ebb and flood tides are summarized in Table II. Whilst mean power density estimates reach 133 and 68 W/m² for ebb and flood tides respectively at location C1, more dynamic location CTb3 presents mean values of approximately 852 and 960 W/m² and maximum reaching over 3,000 W/m² for both ebb and flood tides. That represents a significant spatial variability in tidal resource

TABLE I
VELOCITY STATISTICS SUMMARY FOR BOTH MEASUREMENT LOCATIONS

Velocities (m/s)	C1		CTb3	
	Ebb	Flood	Ebb	Flood
Maximum	1.55	1.28	3.20	3.19
Mean	0.64	0.51	1.18	1.23
Std	0.32	0.26	0.34	0.37
Mean direction (°)	110.97	272.82	99.22	305.33
Std direction(°)	18.86	26.16	23.39	16.61
Asymmetry (°)	18.15		26.11	

TABLE II
POWER DENSITY ESTIMATES FOR BOTH MEASUREMENT LOCATIONS

Power density (W/m²)	C1		CTb3	
	Ebb	Flood	Ebb	Flood
Maximum	1,888	1,064	>3,000	>3,000
Mean	133	68	852	960

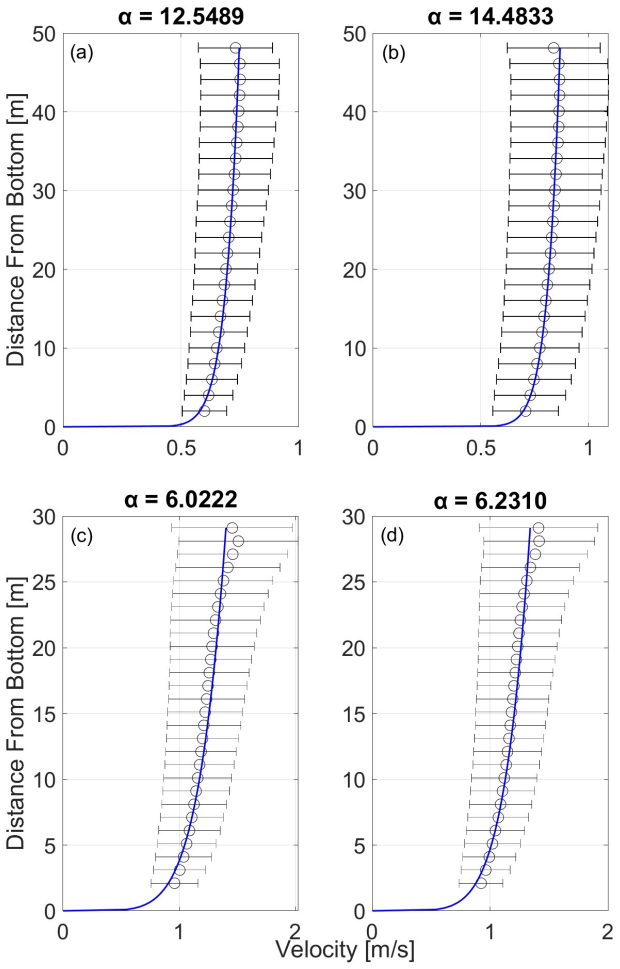

Fig. 6. Average speed profiles for (a) flood and (b) ebb tides from instrument C1 and (c) flood and (d) ebb tides from instrument CTb3. Circles stand for average velocities, black lines stand for the standard deviation and blue line stands for the power law curve fit.

between sites within the channel. Fig. 6 shows the power density distribution over deployment time for both locations. At CTb3 power densities are considerably higher and do not vary substantially between ebb and flood tides. In contrast, C1 presents a more significant variation, with higher values occurring during ebb tide.

In order to appropriately illustrate velocity variations along time, a three-week period – between the 16th May and the 7th June – including spring and neap tides as well as high and low velocity events was selected and results were compared for both locations. Fig 7 shows tidal range, current velocity and direction for this representative time interval for instrument C1. Maximum velocity (1.55 m/s) was measured on the 19th May, during spring tide. Between the 29th May and 7th June, period of neap tide, maximum velocity reached 1.22 m/s on the 2nd June. Yet, for instrument CTb3, velocities during the same period were substantially higher (Fig 8). Maximum velocity during spring tide in this period (3.18 m/s) was recorded on the 17th May. The maximum velocity recorded during neap tide during this time interval happened on the 7th June and was equal to 3.10 m/s.

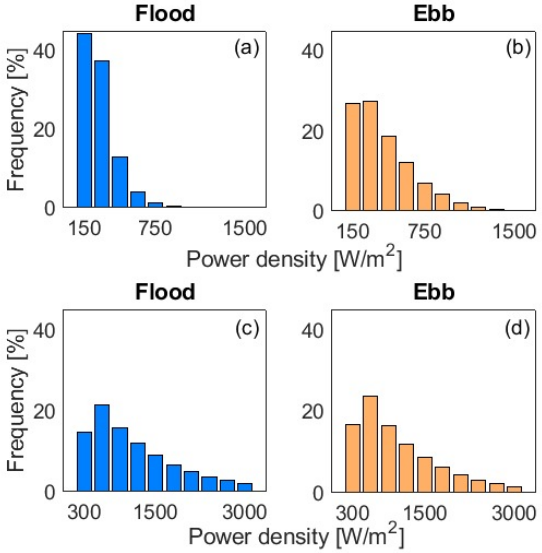

Fig. 5. Power density distribution for location C1 (a)(b) and CTb3 (c)(d) for flood and ebb tides. Velocities classified as slack conditions (30% lowest) were not included in the estimates.

IV. TURBULENCE CHARACTERIZATION AND WAVE-CURRENT INTERACTION

Converting the velocity signal into the frequency domain makes it possible to better estimate the measurement noise floor. Acoustic instruments present intrinsic errors, resulting from the estimation of the Doppler shift, that are typically higher in ADCPs compared to ADVs and visible at high frequency bands of the spectrum [17]. Considering the concept of the turbulent energy cascade, high-frequency eddies of length scales smaller than the Kolmogorov length scale represent dissipation of kinetic energy into heat due to viscosity effects [18]. The presence of noise in turbulence measurements makes it difficult to distinguish bands where viscosity becomes dominant over inertial forces from instrument noise floor, requiring accurate noise estimation methods.

Kinetic energy spectra from 15-minute burst measurements taken on the 22nd May (a) and the 6th June (b), during high velocities at flood tide during spring and neap periods respectively were estimated from stream-wise horizontal velocities. Fig 9 illustrates the spectra for three different depths around hub height (~15 m above the bottom). The energy spectrum from spring tide presents a large peak at the approximate frequency of 0.13 Hz, in the middle of the theoretical inertial subrange. Yet, the graph from the 6th June (Fig 9b) presents a less accentuated peak at a similar frequency, more pronounced 20m above the bottom (the dark blue curve), and is therefore closer to the expected -5/3 slope of the turbulent energy cascade in the inertial subrange.

Stream-wise horizontal velocities measured at high frequency for both 15-min intervals are plotted in Fig. 10. It is evident that velocity fluctuations are higher during spring tide (Fig. 10a), when the largest peak in the kinetic

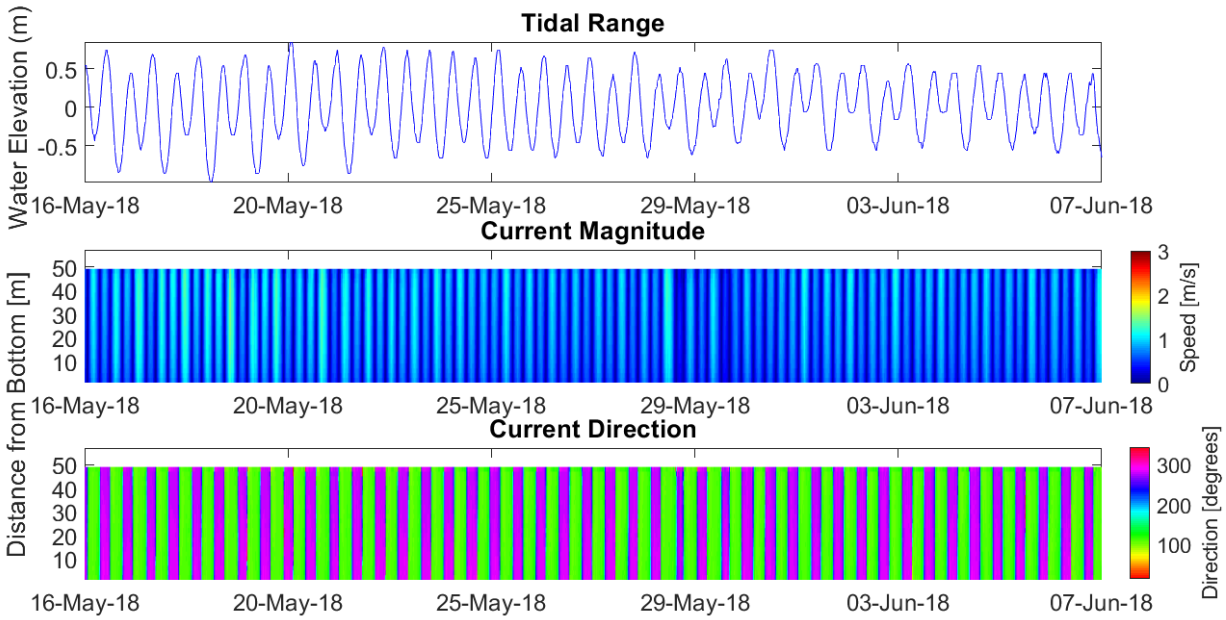

Fig. 7. Tidal range, current magnitude and current direction from instrument C1 measured between 16th May - 7th June, including spring and neap tides as well as high and low velocity events.

energy spectrum is observed. In addition, both figures show variation patterns, e.g. a high frequency velocity fluctuation, related to turbulence, and a low frequency fluctuation, which is related to wave energy, causing the peaks in the energy spectra (~ 0.1 Hz).

Previous studies have observed similar behaviour in the kinetic energy spectra and velocity fluctuations, which has also been attributed to waves (e.g. [19], [20], [21]). Between the 17th – 22nd May high velocities were measured in both instruments and strong wave interference was observed in the kinetic energy spectrum. These results are likely related to strong wind events. Even though the level of interaction varied, as shown in Fig 9, considerable wave-current interaction was observed in most of the data set.

The presence of large peaks in low frequencies is observed at three different depths (15, 20 and 25 m above the bottom), indicating strong wave-current interaction, even at larger depths (dark blue). Wavelength can be estimated based on the wave frequency using:

$$L = \frac{gT^2}{2\pi} \tag{3}$$

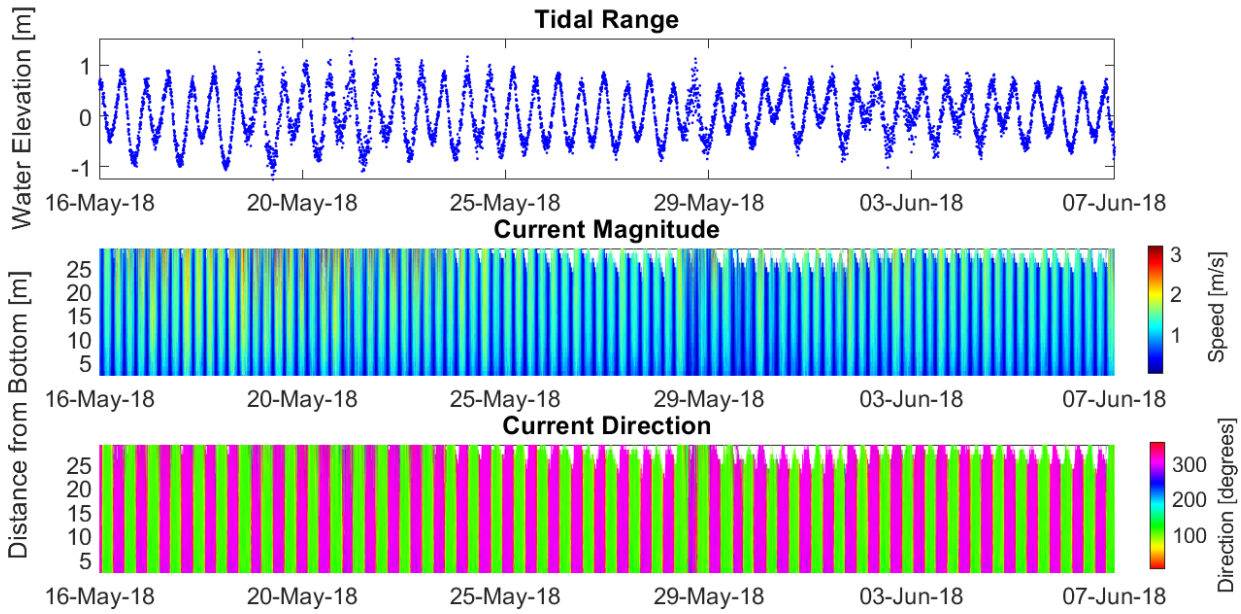

Fig. 8. Tidal range, current magnitude and current direction from instrument CTb3 measured between 16th May - 7th June, including spring and neap tides as well as high and low velocity events.

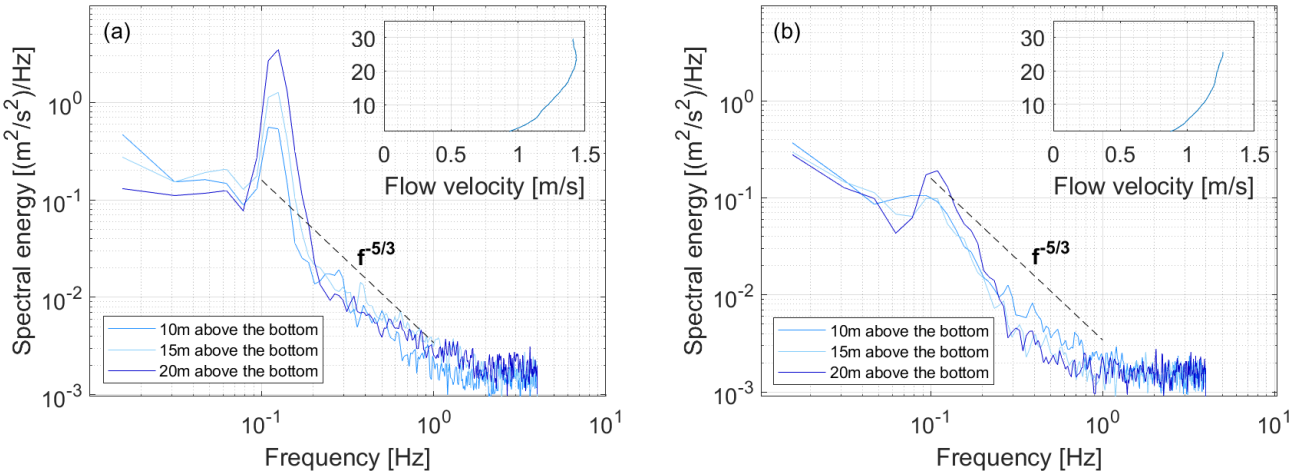

Fig. 9. Kinetic energy spectra from 15-minute burst at three different depths taken by instrument CTb3 on the (a) 22nd May – spring tide – and (b) 6th June – neap tide. Both measurements were taken during fully developed flood tide and show wave interference.

where L is the wavelength, g is the gravity acceleration and T is the wave period, which is the inverse of the frequency. The peak frequencies on spring and neap tide 20 metres above the bottom were 0.13 and 0.11 Hz respectively, resulting in wavelengths of approximately 92.4 and 129.0 m, suggesting wave interference throughout the water column.

For instance, a range of laboratory tests investigated the impact of gravity waves on tidal turbines performance (e. g. [5], [9], [13], [14], [22]). Results have shown that these conditions considerably increase the standard deviation of power, thrust and torque, which may cause additional loading to turbine blades [14]. Similarly, tests in a recirculating water channel demonstrated that mean values of power and thrust in conditions with and without waves are similar. However, under wave influence, these parameters showed large fluctuations, that were observed in the same frequency of the generated waves [5]. In the study presented in [9], the authors have tested the impact of waves from different angles and have reached similar conclusions: the presence of waves does not have a significant impact on mean torque and thrust coefficients, but it considerably increases standard deviations, which could be detrimental for tidal turbine structures. In the work described in [23], laboratory experiments led to the conclusion that unsteady loading derived from wave-current interaction can be attenuated by adjusting turbine blade pitch angle.

In addition to laboratory work, wave-current interaction was found to be a characteristic in other tidal energy sites. The coupled wave and tidal current model developed for the Fall of Warness, Orkney islands, has found wave parameters to be highly influenced by tidal flow, therefore resulting in strong wave-current interaction [6]. In [7] the tidal resource complexity in Cook Strait, New Zealand, has been assessed and wave-current interaction has been detected. This characteristic has been pointed to have implications for vessel operations as well as near-surface structures.

In order to avoid or reduce turbine damage caused by unsteady loading, it is essential to fully characterize tidal resource and flow conditions in the site of interest. Considering the potential for tidal stream energy generation in Banks Straits, the results from the mentioned studies, added to the findings of the present research, reinforce the need to further investigate flow and wave conditions and its spatial variability in this site, as well as the performance of tidal turbines under the observed conditions.

V. Classic ADCPs and New Technology AD2CPs

The data presented here was provided from instruments of different technologies. While the RDI WorkHorse has been used for years to characterize flow

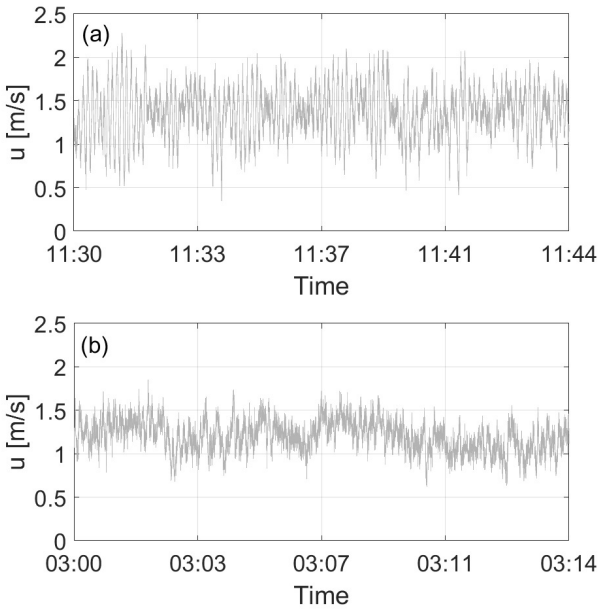

Fig. 10. Stream-wise horizontal velocities measured at 8Hz at CTb3 on the (a) 22nd May, at spring tide, and (b) 6th June, at neap tide, during flood tide.

velocities in various environments, the Norterk AD2CP Signature series has only more recently been introduced to the market. Both instruments have shown to be able to provide good quality velocity data, which is possible to offer tidal developers preliminary information regarding resource characterization, such as velocity profiles and power densities. However, the RDI could not detect the wave-current interaction present in Banks Straits, under the configurations and deployment time described here. The fact that the AD2CP technology allows for dual plan measurements, which resulted in both velocity and turbulence information from a single instrument, has made a significant difference in the site characterization done in this study. Since the EMEC guidelines for tidal stream site characterization recommend the assessment not only of flow velocities but also of turbulence intensities, with the aid of numerical models, the AD2CP instrument is then more appropriate and able to evaluate the performance of turbulence models. There are other ADCP instruments in the market – such as the RDI Sentinel V, measuring at up to 4Hz - capable of measuring turbulence across the water column. However, these are limited by lower sampling rates than the one used by the Signature, which can measure at up to 16Hz. Moreover, the use of a high sampling frequency instrument has enabled turbulence characterization at different water depths and observation of different turbulence frequencies. This has made it possible to obtain further understanding of the extent of the impact of waves in the flow velocities. Obtaining turbulence measurements across the water profile over long deployments, such as the one described here, also allows for estimating the amount of turbulent kinetic energy and the turbulence intensity in the flow at various depths and during different seasons and weather conditions.

VI. FURTHER RESEARCH

The AUSTEn Project, to which this work is part of, has enabled the deployment, during the same period, of a range of different instruments at different locations along Banks Strait. In order to obtain a more detailed tidal resource characterization and fully understand its spatial variability, part of further work is to assess and compare the data collected by other instruments during this three-month period, including velocity, turbulence and wave information. The project also aims to use this data to validate numerical models as well as gain further understanding of sediment transport in the area.

Considering the strong wave-current interaction observed in Banks Strait, to assess turbulence model parameters, such as turbulent kinetic energy and turbulence intensity, it is necessary to decompose wave-turbulence from the velocity signal. There is a range of different methods for this decomposition (e.g. [19], [21], [24]). Part of the proposed future work is to apply and compare different existing wave-turbulence decomposition methods and investigate its advantages and disadvantages in the context of tidal resource characterization. In addition, modelling techniques are important in order to investigate the performance of tidal turbines under the current and wave conditions observed in Banks Strait. Finally, priority sites for turbine micrositing will be identified within Banks Straits.

VII. CONCLUSION

Two instruments with different settings were used in order to characterize velocities and turbulence in Banks Strait. Maximum velocities reached up to 3.20 m/s in the shallower measurement location and 1.55 m/s in the deep pocket. Flow direction varies between the two sites, mostly during flood tide (~32.51°). Mean power density estimates reached up to 133 W/m² at location C1 and over 850 W/m² both during ebb and flood tides at the shallower location, indicating a substantial spatial variability within the channel.

Strong wave-current interaction can be observed even at larger depths during most of the deployment period, which indicates that wave interference is a significant feature in Banks Strait.

The Nortek Signature 1000 kHz (CTb3) was successful in characterizing simultaneously velocity and turbulence along all the water column, which would typically require the use of more than one instrument. High wave-current interaction was observed and would not have been detected by the RDI only, using the configurations described here. In that sense, the possibility of sampling in two different settings, as allowed by the AD2CP technology, has enabled a more detailed site characterization.

REFERENCES

[1] (2018). *Australian Energy Statistics, Table O*.

[2] O. Ellabban, H. Abu-Rub, and F. Blaabjerg, "Renewable energy resources: Current status, future prospects and their enabling technology," *Renewable and Sustainable Energy Reviews,* vol. 39, no. C, pp. 748-764, 2014.

[3] I. A. Milne, A. H. Day, R. N. Sharma, and R. G. J. Flay, "The characterisation of the hydrodynamic loads on tidal turbines due to turbulence," *Renewable and Sustainable Energy Reviews,* vol. 56, no. C, pp. 851-864, 2016.

[4] A. Y. Shcherbina, E. A. D'Asaro, S. J. J. o. A. Nylund, and O. Technology, "Observing Finescale Oceanic Velocity Structure with an Autonomous Nortek Acoustic Doppler Current Profiler," vol. 35, no. 2, pp. 411-427, 2018.

[5] T. A. de Jesus Henriques *et al.*, "The effects of wave–current interaction on the performance of a model horizontal axis tidal turbine," *International Journal of Marine Energy,* vol. 8, no. C, pp. 17-35, 2014.

[6] V. Venugopal, A. Vögler, and B. Sellar, "Characterisation of Wave-Tidal Current-Turbulence Interactions at Tidal Energy Sites in the Orkney Islands," in *The 28th International Ocean and Polar Engineering Conference*, 2018: International Society of Offshore and Polar Engineers.

[7] C. L. Stevens, M. J. Smith, B. Grant, C. L. Stewart, and T. Divett, "Tidal energy resource complexity in a large strait: The Karori Rip, Cook Strait," *Continental Shelf Research,* vol. 33, pp. 100-109, 2012.

[8] J.-F. Filipot, M. Prevosto, C. Maisondieu, M. Le Boulluec, and J. Thomson, "Wave and turbulence measurements at a tidal energy site," ed, 2015, pp. 1-9.

[9] R. Martinez, G. S. Payne, and T. Bruce, "The effects of oblique waves and currents on the loadings and performance of tidal turbines," *Ocean Engineering,* vol. 164, pp. 55-64, 2018.

[10] P. Ouro, M. Harrold, T. Stoesser, and P. Bromley, "Hydrodynamic loadings on a horizontal axis tidal turbine prototype," *Journal of Fluids and Structures,* vol. 71, pp. 78-95, 2017.

[11] T. Blackmore, L. E. Myers, and A. S. Bahaj, "Effects of turbulence on tidal turbines: Implications to performance, blade loads, and condition monitoring," *International Journal of Marine Energy,* vol. 14, no. C, pp. 1-26, 2016.

[12] P. Mycek, B. Gaurier, G. Germain, G. Pinon, and E. Rivoalen, "Experimental study of the turbulence intensity effects on marine current turbines behaviour. Part I: One single turbine," *Renewable Energy,* vol. 66, no. C, pp. 729-746, 2014.

[13] N. Barltrop, K. Varyani, A. Grant, D. Clelland, X. J. P. o. t. I. o. M. E. Pham, Part A: Journal of Power, and Energy, "Investigation into wave—current interactions in marine current turbines," vol. 221, no. 2, pp. 233-242, 2007.

[14] B. Gaurier, P. Davies, A. Deuff, and G. Germain, "Flume tank characterization of marine current turbine blade behaviour under current and wave loading," *Flume tank characterization of marine current turbine blade behaviour under current and wave loading,* vol. 59, pp. 1-12, 2013.

[15] S. Behrens *et al.*, "Ocean renewable energy: 2015–2050. An analysis of ocean energy in Australia," ed: Commonwealth Scientific and Industrial Research Organisation (CSIRO), 2012.

[16] R. Rahimi, I. Penesis, M. Hemer, L. Mason, and G. J. R. E. Thomas, "Characterization of the tidal current resource in Tasmania," vol. 2015, p. 2050, 2014.

[17] J. Thomson, B. Polagye, V. Durgesh, and M. C. Richmond, "Measurements of Turbulence at Two Tidal Energy Sites in Puget Sound, WA," *IEEE Journal of Oceanic Engineering,* vol. 37, no. 3, pp. 363-374, 2012.

[18] S. A. Thorpe, *An Introduction to Ocean Turbulence*. Cambridge, UNITED KINGDOM: Cambridge University Press, 2007.

[19] C. Bian, Z. Liu, Y. Huang, L. Zhao, and W. Jiang, "On Estimating Turbulent Reynolds Stress in Wavy Aquatic Environment," *Journal of Geophysical Research: Oceans,* vol. 123, no. 4, pp. 3060-3071, 2018.

[20] J. P. Newgard and A. E. Hay, "Turbulence intensity in the wave boundary layer and bottom friction under (mainly) flat bed conditions," *Journal of Geophysical Research: Oceans,* vol. 112, no. C9, pp. n/a-n/a, 2007.

[21] J. D. Bricker and S. G. Monismith, "Spectral wave-turbulence decomposition," *Journal of Atmospheric and Oceanic Technology,* vol. 24, no. 8, pp. 1479-1487, 2007.

[22] I. A. Milne, A. H. Day, R. N. Sharma, and R. G. J. Flay, "Blade loads on tidal turbines in planar oscillatory flow," *Ocean Engineering,* vol. 60, no. C, 2012.

[23] T. A. de Jesus Henriques, T. S. Hedges, I. Owen, and R. J. Poole, "The influence of blade pitch angle on the performance of a model horizontal axis tidal stream turbine operating under wave–current interaction," *Energy,* vol. 102, no. C, pp. 166-175, 2016.

[24] C. Smyth, A. E. Hay, and L. Zedel, "Coherent Doppler Profiler measurements of near-bed suspended sediment fluxes and the influence of bed forms," *Journal of Geophysical Research: Oceans,* vol. 107, no. C8, pp. 19-1-19-20, 2002.